



Geostatistical modeling of surface water balance (SWB) under variable soil moisture conditions in the Pao river basin, Venezuela

Bettys Farías ^a, Adriana Marquez ^a, Edilberto Guevara ^a & Demetrio Rey ^b

^a Facultad de Ingeniería, Universidad de Carabobo, Carabobo, Venezuela., bettysfarias@gmail.com, ammarquez@uc.edu.ve, eguevara@uc.edu.ve

^b Instituto de Matemática y Computo Aplicado, Universidad de Carabobo, Carabobo, Venezuela, drey@uc.edu.ve

Received: June 15th, 2019. Received in revised form: March 3rd, 2020. Accepted: April 15th, 2020

Abstract

The aim of this paper is to develop a geostatistical model for the surface water balance (SWB) under variable soil moisture conditions of the Pao river basin, Venezuela. The novelty of the research consists in identifying a statistical model that will predict the spatial variability of hydro-meteorological data in the basin. A series of meteorological data from 25 stations for the period 2015-2017 were used in connection with the ordinary kriging technique. Infiltration values were analyzed considering three different soil moisture conditions: dry, normal and wet. To represent the semi variances of the SWB variables, the function J-Bessel was used. An adequate mathematical adjustment between observed and predicted values of SWB variables has been found expressed by the correlation coefficient (R) as follows: for precipitation, 0.54-0.81; for infiltration, 0.68-0.95; for runoff, 0.68-0.92; for evapotranspiration, 0.53-0.86; and for the accumulative volume, 0.53-0.95.

Keywords: Geostatistics modeling; kriging; semivariance analysis; water balance; infiltration; soil moisture.

Modelación geoestadística del balance hídrico superficial (BHS) bajo condiciones variables de humedad del suelo en la cuenca del río Pao, Venezuela

Resumen

El objetivo de este trabajo es desarrollar un modelo geoestadístico para la estimación del balance hídrico superficial (BHS) bajo condiciones de humedad variable en la cuenca del río Pao, Venezuela. Lo novedoso de la investigación consiste en identificar un modelo estadístico que prediga la variabilidad espacial de los datos hidrometeorológicos en la cuenca. Se utilizan series de datos meteorológicos de 25 estaciones para el período 2015-2017 y la técnica de kriging ordinaria. La variable infiltración se analizó para diferentes condiciones de humedad del suelo: seco, normal y húmedo. Para representar las semi varianzas de las variables hidrometeorológicas, se utilizó la función J-Bessel. Se ha encontrado un ajuste matemático adecuado entre los valores observados y estimados de las variables del balance hídrico expresados por el coeficiente de correlación (R), habiendo obtenido los siguientes rangos: para precipitaciones, 0.54-0.81; para la infiltración, 0.68-0.95; para escorrentía, 0.68-0.92; para evapotranspiración, 0.53-0.86; y para el volumen acumulativo, 0.53-0.95.

Palabras clave: modelación geoestadística; krigado; análisis de semi varianza; balance hídrico; infiltración; humedad del suelo.

1. Introduction

One of the most influential variables in the process of establishing watershed water balance is surface runoff -- the sheet of water from rainfall which does not seep into the soil and drains onto the surface and that depending on the state

and characteristics of the basin moves at different speeds causing various negative effects on watershed management, such as erosion and floods [1]. For this reason, hydrometeorological, hydrological, hydraulic, economic, social and political principles must be integrated into the analysis.

How to cite: Fariás, B, Marquez,A, Guevara, E. and Rey, D, Geostatistical modeling of surface water balance (SWB) under variable soil moisture conditions in the Pao river basin, Venezuela. DYNA, 87(213), pp. 192-201, April - June, 2020.

Each basin has unique features that identify and differentiates it from its environment. However, the hydrological processes that develop in each one is similar: precipitation, infiltration, evapotranspiration, and runoff. Precipitation is one of the main climatic variables required for the estimation of water balance; it significantly influences climatic phenomena that may be adverse to society, such as floods.

Modeling and simulation of water balance and flooding variables require the use of technological tools that allow us to distinguish the probable causes of the damage caused in the basin and thus to document the key factors involved in such damages. Among these tools are the hydrodynamic and rainfall-runoff models, which permit to simulate the influence of the spatial distribution of water balance variables and natural properties of the basin on runoff processes [2, 3]. These models are used in combination with geographic information systems (GIS), expanding the range of hydrological investigations, and therefore, the understanding of the fundamental physics of the hydrological cycle processes and the solution of mathematical equations that represent these processes.

In addition, hydrodynamic models can be combined with interpolation methods that allow the interaction of topographical and geographical data, which have been used in various parts of the world to generate maps of water balance variables [4, 5, 6]. These methods use multivariate statistical models that allow evaluating the relationship of climate data with geographical and topographical variables of weather stations and their spatial correlation [5, 6].

This study aims to establish a geostatistical model to predict the magnitude and location of the hydrometeorological variables involved in water balance as precipitation, evapotranspiration, infiltration, runoff and the volume of water stored, including the evaluation of the incidence of antecedent soil moisture conditions in surface runoff produced in the basin.

Estimation of runoff is of great interest for various applications: environmental impact studies, land use planning, management of watersheds and natural resources, prediction of flood risks and implementation of early warning systems [7].

The results of this research will provide basic input for designing a Risk Management Flood Plan, and its implementation will be useful in preventing damage to communities which are located in the flood plains of the 14 main rivers as in the surrounding areas of the three water reservoirs of this basin and that constitute the supply system of the central region of country.

2. Methodology

2.1. Study area

The Pao River basin is located in the North-Central region of the Bolivarian Republic of Venezuela. It has a territorial extension of 3.019 km², distributed among the states of Carabobo, Cojedes and Guárico. It lies between North

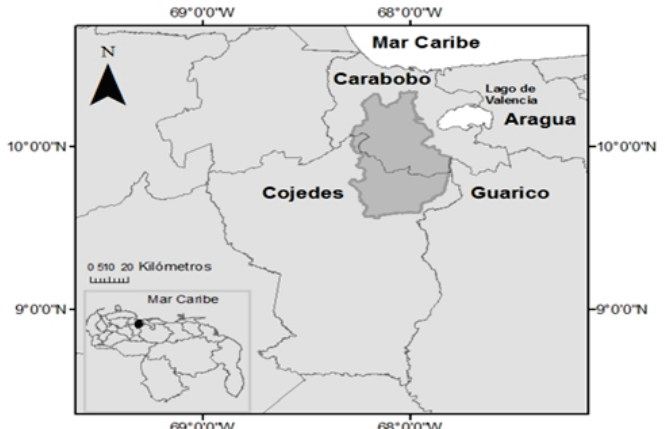


Figure 1. Geographical location of the Pao River basin in the North-Central region of the Bolivarian Republic of Venezuela by the Caribbean Sea.
Source: MANR

latitudes 9° 33'38.991", 10° 20' 29.963, and West longitudes 68° 17'35.54", 67° 48' 319.348" [8, 9]. The geographical location of the Pao River basin in the North-Central region of the Bolivarian Republic of Venezuela by the Caribbean Sea is shown in Fig. 1.

The research was carried out in two phases. Phase I involves the geostatistical modeling and Phase II comprises the spatio-temporal modeling of water balance variables of the Pao River basin.

The activities in each phase are described as follows:

2.2. Phase I: geostatistical modeling

The application of geostatistical techniques requires complying with the following steps: 1. Exploratory Analysis, 2. Structural Analysis, 3. Predictions [10].

Using an exploratory analysis, the compliance with the principles of stationarity and extreme outliers are verified, data normality by transformations, evaluation of variable distribution and the existence of correlations among them are identified. The module of Geostatistical Analysis in ArcGis 10.0, is used for producing histograms and determining if the data are fitted a normal distribution function. For a Gaussian distribution of data, the mean and median must be similar, a unit difference between them is accepted. The bias coefficient must be a value between 0 and 0.5. If this is not fulfilled, the data must be transformed [11].

The structural analysis consists of analyzing data to determine its spatial variability, evaluating the presence of anisotropy, and determining variogram models (graphs) for each variable, followed by its validation using the cross-validation technique [12].

By using structural analysis, theoretical models are adjusted to represent the spatial correlation between data (semivariograms), and by using spatial interpolation techniques kriging, the value assumed by the study variables for different points within the region is estimated [13].

In this research, ordinary kriging method was selected,

which has been used to model hydrometeorological data in other studies.

The ordinary kriging method is the best linear unbiased estimator, turning it into the optimal technique for the interpolation of any type of spatial variable [14].

The advantage of the ordinary kriging method is the possibility of modeling the spatial dependence of data, and thus, provides the best results among other purely spatial methods in the interpolation of precipitation [15, 16].

The method of ordinary kriging has been used for the application of radar rainfall data for estimating field precipitations for climate purposes. These are some examples of the application of the ordinary kriging estimator as an adequate statistical interpolation method to reliably estimate precipitation values.

The data are represented in an empirical semivariogram and the mathematical models used for their theoretical representation (curve) correspond to Circular, Spherical, Exponential, Gaussian, Bessel-J, K-Bessel, and Stable models, for being the ones commonly employed.

The final step in the geostatistical analysis was forecasting. The setting of the experimental variograms always causes uncertainty on the stationarity assumptions and selected models among others, which contribute to errors in estimation. Therefore, a means to diagnose some problems in the retrieved setting is the use of cross-validation, whose basic idea is to delete a datum in order to predict the deleted observations. If the chosen theoretical model is good or adequately describes the spatial dependence, the predicted value will be close to the real one [17].

The model to be selected is the one that best reproduces the known data; and therefore, will comply with the following conditions: root mean square error (RMSE): the smaller, the better forecasting; standard error of the mean (SEM): small, close to RMSE; the variability of the prediction is calculated correctly and the root mean square error (RMSE): near one (1). If this is fulfilled, the forecast errors are valid.

2.3. Phase II: Modeling of water balance variables

2.3.1. Data Collection

Meteorological data:

The weather information used in this research is taken from 25 monitoring stations at the six States surrounding the basin, property of the National Institute of Meteorology and Hydrology (INAMEH for its acronym in Spanish).

The data was obtained from the website of institute from January 2015 to December 2017, presented in Table 1.

Satellite data:

Satellite information was taken from the Landsat satellites L8OLI, for the years 2015, 2016 and 2017, respectively, 36 satellite images were obtained from the web page <https://earthexplorer.usgs.gov/> of the United States Geological Service (USGS). The scene used for the Pao River basin is identified under the global reference system according to the following row and path: 005 and 053, respectively.

Table 1
Telemetry control network of weather stations in the basin of the Pao River, States of Carabobo, Aragua, Cojedes, Guárico, Federal District and Falcon.

N	Projected Coordinates UTM Zone 19 N	Name of Station	State
1	613822	Hda Manglar	Carabobo
2	616988	San Diego	Carabobo
3	622148	Guacara	Carabobo
4	592724	Cpo Carabobo	Carabobo
5	622892	Vigirima	Carabobo
6	626026	Aguia Blanca	Carabobo
7	608178	Valencia-Ofna	Carabobo
8	619290	Potabilizadora	Carabobo
9	598708	Guataparo	Carabobo
10	603183	Guaparo- Café	Carabobo
11	689996	San Fco del Pao	Aragua
12	727848	Valle Morin	Aragua
13	701139	San Sebastian	Aragua
14	690407	Quebrada Seca	Aragua
15	674382	El Cortijo	Aragua
16	677672	La Yeguera	Guárico
17	688034	Ortiz	Guárico
18	677610	Los Morros	Guárico
19	677610	Tinaquillo	Cojedes
20	548113	Unellez	Cojedes
21	546523	S.C Aeropuerto	Cojedes
22	735254	La Carlota	D. Federal
23	753237	Los Roques	D. Federal
24	814161	La Orchila	D. Federal
25	460647	Pto Cumarebo	Falcón

Source: INAMEH

The map projection parameters according to the USGS are: 1) Projection: UTM, 2) Datum: WGS1984, 3) Ellipsoid: WGS84, 4) UTM Zone: 19 N, 5) cubic convolution as the resampling method.

The data corresponding to the identification and date of acquisition of the satellite images downloaded from the satellite Landsat L8OLI, for the period January - December 2015 are presented in Table 2. As a sample, the identification of the image of satellite Landsat 8 OLI acquired in 2015-01-15 corresponds to the following identification LC80050532015015LGN01.

2.3.2. Data Processing

This study required the use of various techniques and computational tools for the preliminary processing of the Landsat satellite images, which include absolute and relative

Table 2.
Characteristics of satellite images from Landsat 8 OLI

N	Identificación	Fecha de Adquisición
1	LC80050532015015LGN01	2015-01-15
2	LC80050532015047LGN01	2015-02-16
3	LC80050532015063LGN01	2015-03-04
4	LC80050532015111LGN01	2015-04-21
5	LC80050532015127LGN00	2015-05-07
6	LC80050532015175LGN01	2015-06-24
7	LC80050532015191LGN01	2015-07-10
8	LC80050532015223LGN01	2015-08-11
9	LC80050532015271LGN01	2015-09-28
10	LC80050532015303LGN01	2015-10-30
11	LC80050532015319LGN01	2015-11-15
12	LC80050532015335LGN01	2015-12-01

Source: The Authors.

corrections of each image. The atmospheric, topographic and radiometric corrections applied to each image were executed with the computational tool of satellite image processing known as ENVI 4.7.

For the change detection of use and land cover (LULC) in the basin of the Pao River during the period 2015-2017, the satellite image processing was applied on a multispectral image pixel, being labeled according to the LULC category to which belong. From each image, it was generated thematic cartography and statistical inventory of the area involved in each category. There are two methods of classification: supervised and unsupervised, supervised classification process was used; this type of classification is based on the prior knowledge of classes and statistics that relate to each spectral class of the image. [18, 19] consists of two (2) phases: training and assignment

In phase 1, it was carried out a general recognition of the study area, determining shapes and colors patterns related to a class. By means of pixel training samples it was possible to classify the whole pixel to its corresponded class. The spectral characteristics of bands allow the discrimination of pixel groups that belong to a same LULC class through the generation of their spectral signatures [20]. In phase 2, a list of names or classes is assigned to each pattern observed, by means of algorithms generating a general classification of the image. Once the classification is executed, it is recommended to verify it. For this, a confusion matrix, which includes unclassified/classified pixels, is used as measurement tool. Three types of accuracy were generated with the confusion matrix: global accuracy, accuracy of the user and accuracy of producer [21], as well as the Kappa index [22]. This process is called image classification and it seems to follow the supervised method.

To obtain the losses and estimate the surface runoff from them, the method of the U.S. Soil Conservation Service was used [23].

This method requires to know the type and use of the basin soil studied to determine curve number, pluviographic records, and other factors such as the time elapsed since the last rainfall and evapotranspiration during the period of study.

In this investigation, water balance was expressed according to the following equation:

$$\Delta S = I - ETR \quad (1)$$

Where ΔS represents the variation of water stored in the soil (mm); I represents the infiltration in (mm); ETR evapotranspiration in (mm). It is considered that

$$I = P - ES \quad (2)$$

Where P represents precipitation (mm); ES represents the surface runoff (mm).

3. Results

The results that encompass the creation of variable maps

Table 3.
Models and forecast errors

Model	M	RM SE	ME D	R		SE M
				MS	M	
1	Circular	0.	1.05	4	0.1	1.6
	Spherical	08	1.02	3	0.1	1.5
	Exponential	09	1.05	3	0.1	1.6
	Gaussian	08	1.02	2	0.1	1.5
	Cuadratic	0.	1.05	3	0.1	1.6
	K-Bessel	0.	1.02	2	0.1	1.5
	J-Bessel	09	1.03	1	0.1	1.5
	Stable	08	1.02	2	0.1	1.5

(RMSE) root mean square error; (SEM) standard error of the mean; (RMS) root mean square (RMS).

Source: The Authors.

using GIS techniques are the following: a) LULC, b) precipitation, c) evapotranspiration, d) infiltration, e) effective precipitation, and (f) storage of water volume.

With regard to the phase I of investigation which corresponds to geostatistical modeling it was observed that the behavior of the data of rainfall reported by the network of weather stations used in this study reported a mean of 16.8 and a median 16.4, with a coefficient of asymmetry of 0.25, which confirms a behavior of normal distribution of the data, the trend that follows the distribution of the data is of second order which. It will be removed in the structural analysis. The behavior of the hydrometeorological variables presented non-stationarity with respect to the X-axis, and y Z. In addition to an anisotropic behavior. Table 3 shows the models and forecast errors.

According to this analysis, the Bessel-J model was selected since it best fitted the values of the variables to be studied in this research.

3.1. Land use and cover

The types of soils present in the basin were determined from the soil map obtained from the website of the Ministry of Environment and Natural Resources prepared for the Bolivarian Republic of Venezuela, the results in Fig 2 show the presence of four types of soil: 1) Oxisol (13.30%), 2) Inceptisol (60.21%), 3) Mollisol (5.92%) and (4) Ultisol (20.5%). As a sample, the mean of the amount of organic carbon at different depths of the profiles in the order inceptisols is varying between 1.1 and 1.44% to 0-15 cm soil depth [24]. The distribution of inceptisol soil particle size corresponds to a depth of 0 to 24 cm determined by [25] corresponds to: sand: 70.45%, silt: 15.06%, clay: 14.49%. The mean amount of organic matter and mean texture [26, 27] determine the type of soil of the mollisols as follows: organic matter: 26 g / kg (2.71%), sand: 120 g / kg (12.5%) silt: 577 g / kg (60.16%), clay: 236 g / kg (24.6%). As it can be seen, the soils of Pao River basin have predominantly

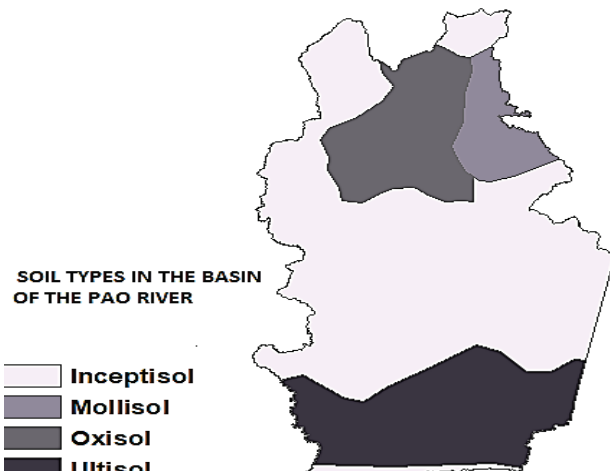


Figure 2. Soil types present in the basin of the Pao River.
Source: The Authors.

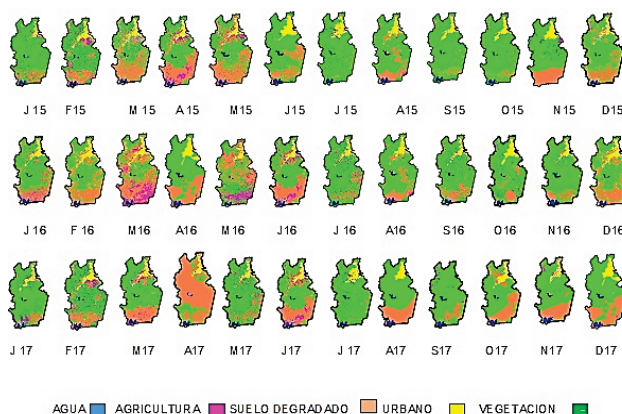


Figure 3. Use and land cover in the basin of the Pao River in the period from 2015-2017.
Source: The Authors.

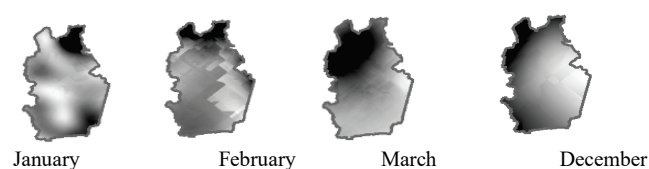
contained particles of fine and finest, being considered as class C (moderately high runoff) and D (high runoff) according to the hydrologic classification of US-SCS.

Fig. 3 shows the results from the application of change detection techniques in areas destined for land use and cover of the Pao River basin corresponding to the post-classification comparison method from January 2015 to December 2017. The result of the kappa index to validate the classification carried out is in the category of satisfactory compared with the level of concordance of [28]. For other authors, kappa represents the value of K or strength of concordance, the retrieved value falls in the range from 0.81 to 1, which is classified as very good.

A more detailed investigation of this use of the Pao River basin land classification can be reviewed in [29].

3.2. Precipitation

The area studied has two climatic seasons [30]: a dry



Precipitation Minimum □ Precipitation Máximo ■
Figure 4. Spatial prediction of monthly precipitation (mm/month) occurring in the Pao River basin in the dry season for 2016.
Source: The Authors.

Table 4.
Results of the spatial prediction statistical modeling of monthly rainfall in the dry season for 2016.

Model	Ordinary Kriging
	January 2016
SPSM	0.02*Nugget+0.02*J-Bessel (27431,10)
RFP	0.55 * x + 0.13
	February 2016
SPSM	0.16*Nugget+0.26*J-Bessel (48347,1.86)
RFP	0.53 * x + 0.21
	March 2016
SPSM	0.12*Nugget+0.12*J-Bessel (55179,0.01)
RFP	0.52 * x + 0.15
	December 2016
SPSM	8.33*Nugget+159.98*J-Bessel (121280,10)
RFP	0.81 * x + 6.68

(SPSM) Spatial prediction statistical model. (RFP) Regression function Prediction.

Source: The Authors.

season corresponding to the months from December to March with low-intensity monthly precipitations ranging from 0 mm/month to 48 mm/month, and a rainy season from April to November with a monthly precipitation varying from 11.58 mm/month to 419.96 mm/month.

Fig. 4 represents a sample of the results from the monthly precipitation in mm/month during the dry season for 2016. It is observed for January (0.095-0.740), February (0.071-0.745), March (0.051-1.669), December (28.31-45.2). For 2016, the mean precipitation was of 13.60 mm/year in the dry season and 282.92 mm/year in the rainy season.

The information shown in Table 4 corresponds to the results of the spatial prediction statistical modeling of precipitation from the dry season in the Pao River basin for 2016.

The spatial prediction statistical model (SPSM) used is the Bessel-J function. The equation is expressed as follows:

$$a * \text{nugget} + b (\text{Bessel} - J(c, d)). \quad (3)$$

Where the coefficient a is associated with the non-spatial correlation; the coefficient b is associated with the term $C_0 + C_1$, which is the threshold variation; the coefficient c represents the maximum distance between neighboring precipitation observation stations; and the coefficient d represents the parameter of the Bessel-J function. The coefficient values vary as follows Table 4: a : between 0.01 and 8.331, b : between 0.0233 and 159.98, c : between 27431 and 121280, d : between 0.01 and 10. A pattern for the

semivariances of the SPSM for the dry season associated with the first months of each year is observed. In all cases, the semivariances are smaller in the shortest distance and then stabilize at a certain distance.

3.3. Evapotranspiration

The area studied has two seasons: a dry season corresponding to the months from December to March with a monthly evapotranspiration presenting a high intensity spatial distribution, which reaches up to 1372.64 mm/month; and a rainy season from April to November with a monthly evapotranspiration ranging from 0.00 mm/month to 3627.8 mm/month.

Fig. 5 represents a sample of the results from the monthly evapotranspiration in mm/month during the dry season for 2016. It is observed for January (0.00-269.35), February (130.40-153.77), March (159.89-185.47), and December (84.68-109). For 2016, the average evapotranspiration was of 179.39 mm/year in the dry season and 134.42 mm/year in the rainy season.

The information shown in Table 5 corresponds to the results of the spatial prediction statistical modeling of evapotranspiration based on the dry season in the Pao River basin for 2016. The spatial prediction statistical model (SPSM) used is the Bessel-J function. The equation is expressed as follows:

$$a * \text{nugget} + b (\text{Bessel} - J(c, d)). \quad (4)$$

Where the coefficient a is associated with the non-spatial correlation; the coefficient b is associated with the term $C_0 + C_1$, which is the threshold variation; the coefficient c represents the maximum distance between neighboring precipitation observation stations; and the coefficient d represents the parameter of the Bessel-J function correlation especially. The coefficient values vary as follows Table 5 a: between 9.658 and 200.81, b: between 59.797 and 830.84, c: between 57539 and 135640, d: between 0.01 and 4.39. A pattern in the SPSMs for the dry season associated with the first months of each year is observed. In all cases, the semivariances are smaller in the shortest distance and then stabilize at a certain distance.

Table 5.
Results of the spatial prediction statistical modeling of the monthly evapotranspiration during the dry season for 2016.

Model	Ordinary Kriging
	January 2016
SPSM	200.81*Nugget+830.84*J-Bessel(135640,2.03)
RFP	0.62 * x + 6.61
	February 2016
SPSM	31.39*Nugget+65.61*J-Bessel(82709,4.39)
RFP	0.56 * x + 62.27
	March 2016
SPSM	18.187*Nugget+150.42*J-Bessel(57539,1.8517)
RFP	0.860 * x + 26.10
	December 2016
SPSM	9.66*Nugget+59.797*J-Bessel(112880,0.01)
RFP	0.532 * x + 42.94

Source: The Authors.

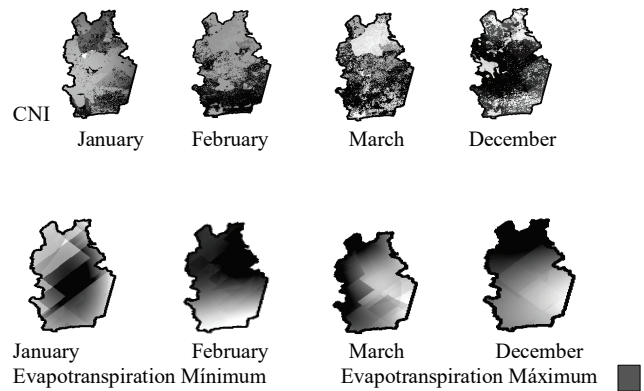


Figure 5. Spatial prediction of monthly evapotranspiration (mm/month) occurring in the Pao River basin during the dry season for 2016.
Source: The Authors.

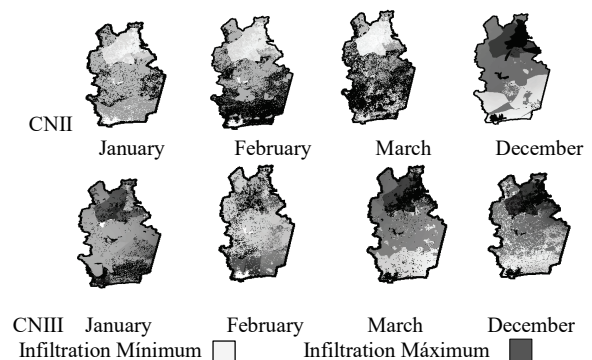


Figure 6. Spatial prediction of monthly infiltration (mm/month) modifying the Pao River basin soil moisture conditions during the dry season for 2017.
Source: The Authors.

3.4. Infiltration

Fig. 6 represents a sample of the results from the monthly infiltration expressed in mm/month for different soil moisture conditions: dry (CNI), normal (CNII) and wet (CNIII). Taking as an example the dry season for 2017, infiltration values are as follows: January: CNI (0.0189-148.245); CNII (0.00-129.54); CNIII (0.0189-91.5297). February: CNI (0.0-43.972); CNII (0.00-25.912); CNIII (0.00 - 26.047). March: CNI (0.00-48.06); CNII (0.00-47.41); CNIII (0.0-45.743). December: CNI (0.00-95.81); CNII (0.00-94.21); CNIII (0.00-73.90). During the rainy season for 2017, an increase in infiltration without any significant differences regarding variations of humidity conditions was observed. The maximum average of infiltration was 227.92 mm.

The information shown in Table 6 corresponds to the results of the spatial prediction statistical modeling of infiltration according to the dry soil moisture condition (CN I) during the dry season in the Pao River basin for 2017.

The spatial prediction statistical model (SPSM) used is the Bessel-J function. The equation is expressed as follows:

$$a * \text{nugget} + b (\text{Bessel} - J(c, d)). \quad (5)$$

Table 6.

Results of the spatial prediction statistical modeling of monthly infiltration during the dry season for 2017.

Model	Ordinary Kriging (CN I)
	January 2017
SPSM	643.4*Nugget+567.76*J-Bessel (22001,4.05)
RFP	0.82 * x + 13.37
	February 2017
SPSM	1469.5*Nugget+323.52*J-Bessel(4202.2,4.82)
RFP	0.69 * x + 4.53
	March 2017
SPSM	18.187*Nugget+150.42*J-Bessel(57539,1.8517)
RFP	0.9105* x + 2.98
	December 2017
SPSM	95.076*Nugget+205.6*J-Bessel(23684,3.51) 0.95*x +
RFP	3.140

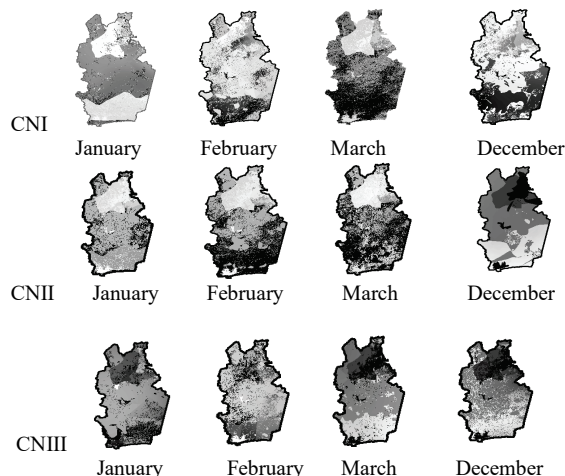
Source: The Authors.

Where the coefficient a is associated with the non-spatial correlation; the coefficient b is associated with the term $C_0 + C_1$, which is the threshold variation; the coefficient c represents the maximum distance between neighboring precipitation observation stations; and the coefficient d represents the parameter of the Bessel-J function. The coefficient values vary as follows Table 6 a: between 26.57 and 1469.5; b: between 29.47 and 567.76 c: between 4202.2 and 23684, d: 3.5148 and 4.82

A pattern in the SPSMs for the dry season associated with the first months of each year is observed. In all cases, the semivariances are smaller in the shortest distance and then stabilize at a certain distance

3.5. Effective precipitation

Fig. 7 represents a sample of the results from the monthly effective precipitation expressed in mm/month for different soil moisture conditions: dry (CNI), normal (CNII) and wet (CNIII).



Effective Precipitation Minimum Effective Precipitation Maximum
Figure 7. Spatial prediction of effective monthly precipitation (mm/month) modifying the Pao River basin soil moisture conditions during the dry season for 2015.

Source: The Authors.

Table 7.

Results of the spatial prediction statistical modeling of monthly runoff during the dry season for 2015.

Model	Ordinary Kriging (CN II)
	January 2015
SPSM	16.62*Nugget+21.92*J-Bessel(25636,10)
RFP	0.90 * x + 0.29
	February 2015
SPSM	13.22*Nugget+34.00*J-Bessel(87850,0.01)
RFP	0.92 * x + 0.63
	March 2015
SPSM	18.21*Nugget+18.874*J-Bessel (85098,0.01)
RFP	0.69 * x + 2.03
	December 2015
SPSM	3.90*Nugget+4.05*J-Bessel(91429,9.22)
RFP	0.75 * x + 0.62

Source: The Authors.

Taking as an example the dry season for 2015, the effective precipitation values are as follows: January: CNI (3.36-34.62); CNII (3.36-25.94); CNIII (0.091-45.5). February: CNI (0.010-45.5); CNII (6.58-45.5); CNIII (0.09-45.5). March: CNI (0.629-28.70); CNII (2.44-14.60); CNIII (0.0-4.656). December: CNI (0.00-45.5); CNII (0.441-22.82); CNIII (0.00-45.5).

During the rainy season for 2015, an increase of effective precipitation without any significant differences regarding variations of humidity conditions was observed. The maximum average of surface runoff was 164.11 mm.

The information shown in Table 7 corresponds to the results of the spatial prediction statistical modeling of runoff according to normal soil moisture conditions (CN II) during the dry season in the Pao River basin for 2015

The spatial prediction statistical model (SPSM) used is the Bessel-J function. The equation is expressed as follows:

$$a * \text{nugget} + b (\text{Bessel} - J(c, d)) \quad (6)$$

Where the coefficient a is associated with the non-spatial correlation; the coefficient b is associated with the term $C_0 + C_1$, which is the threshold variation; the coefficient c represents the maximum distance between neighboring precipitation observation stations, and the coefficient d represents the parameter of the Bessel-J function.

The coefficient values vary as follows Table 7 a: between 3.90 and 18.21, b: between 4.05 and 34.00, c: between 25636 and 91429, d: between 0.01 and 10. A pattern in the SPSMs for the dry season associated with the first months of each year is observed. In all cases, the semivariances are smaller in the shortest distance and then stabilize at a certain distance.

3.6. Storage of water volume

Fig. 8 represents a sample of the results from the monthly storage of water volume expressed in mm/month for different soil moisture conditions: dry (CNI), normal (CNII) and wet (CNIII).

Taking as an example the dry season for 2016, storage of water volume values are as follows: January: CNI (- 2.693-21.0); CNII (- 2.693-21.0); CNIII (- 2.693-21.0). February:

CNI (- 153.7, - 130.4); CNII (- 153.7, - 130.4); CNIII (- 153.7, - 130.4). March: CNI (- 185.4, - 159.8); CNII (- 185.4, - 159.8); CNIII (- 185.4, - 159.8). December: CNI (- 109.8 - 84.68); CNII (- 109.8, 84.68-); CNIII (- 109.8, - 84.68).

During the rainy season for 2016, an increase in the storage of water volume without any significant differences regarding variations in humidity conditions was observed. The maximum average of storage of water volume was - 88.46 mm.

The results presented a storage deficit in this basin for 2016 and 2017.

The information shown in Table 8 corresponds to the results of the spatial prediction statistical modeling of the monthly storage of water volume during the dry season in the Pao River basin for 2016.

The spatial prediction statistical model (SPSM) used is the Bessel-J function. The equation is expressed as follows:

$$a * \text{nugget} + b (\text{Bessel} - J(c, d)) \quad (7)$$

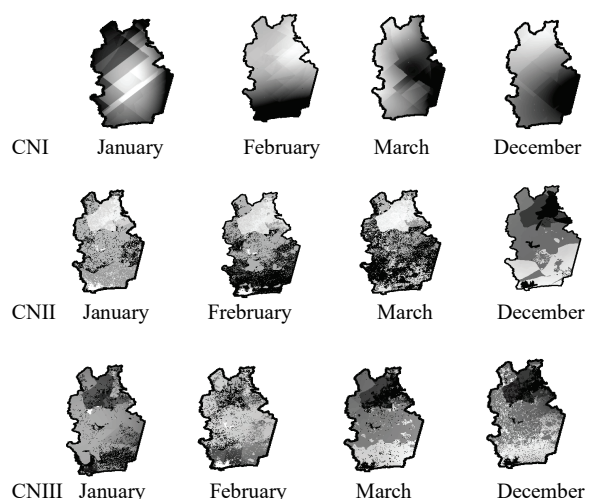


Figure 8. Spatial prediction of monthly storage of water volume (mm/month) modifying the Pao River basin soil moisture conditions during the dry season for 2016.

Source: The Authors.

Table 8.
Results of the spatial prediction statistical modeling of the monthly storage of water volume during the dry season for 2016

Model	Ordinary Kriging (CN II)
	January 2016
SPSM	263.63*Nugget+ 131.56*J-Bessel(48774,0.63)
RFP	0.68* x + 15.32
	February 2016
SPSM	40.97*Nugget+55.57*J-Bessel(99638,0.01)
RFP	0.78 * x + 5.20
	March 2016
SPSM	29.52*Nugget+14.91*J-Bessel (76765,0.01)
RFP	0.65* x + 2.03
	December 2015
SPSM	0*Nugget+10.32*J-Bessel(316.75,3.03)
RFP	0.96* x + 0.19

Source: The Authors.

Where the coefficient a is associated with the non-spatial correlation, the coefficient b is associated with the term $C_0 + C_1$, which is the threshold variation the coefficient c represents the maximum distance between neighboring precipitation observation stations, and the coefficient d represents the parameter of the Bessel-J function.

The coefficient values vary as follows Table 8 a: between 0 and 263.63, b: between 10.32 and 131.56, c: between 316.75 and 99638, d: between 0.01 and 3.03.

A pattern in the SPSMs for the dry season associated with the first months of each year is observed. In all cases, the semivariances are smaller in the shortest distance and then stabilize at a certain distance.

4. Discussion of results

The post-classification comparison method results in five classes: a) water, b) agriculture, c) degraded soil, d) vegetation and e) urban area. The Pao River basin shows the presence of vegetation with 75.43%, represented by bushes, forests and natural grasslands grazed [31], and agricultural use 12% as classes predominantly during the rainy season, while average urban area in 3.7% and 1% water. While the dry season is dominated by the presence of degraded soils by 55%, 8% agricultural use, the urban area is maintained at an average of 3.6% and water at 0.8%.

The existence of degraded soils as a result of indiscriminate deforestation for traditional farming of smallholdings that has led to a loss of the original vegetation cover was observed [32].

Regarding precipitation, the results show that the rainy season concentrates more than 85% of the total annual precipitation, while in the dry months it barely rains with a monthly precipitation below the reference evapotranspiration [33].

Monthly watershed infiltration was evaluated according to soil moisture conditions: condition I for dry soil, condition II for normal soil, and condition III for moist soil. During the period studied in this research, the infiltration parameter values obtained are low, closer to the minimum value. No significant differences in accordance with diverse soil moisture conditions are observed [34].

In the basin of the Pao River, for the purposes of estimation of infiltration and runoff most of the area is occupied with soil organic silt, silty sand and silty clay that corresponds to soils of moderate potential for runoff (hydrological groups C and D) the values from the variable surface runoff makes that the relative grade it means almost throughout the basin, which responds to the vegetation cover in rainy season and the reported values deficit of storage in the basin [31].

Runoff values range from 0.0 to 370 mm / year in 2015; 0.0mm to 389 mm/year in 2016, and 0.0 to 312 mm per year in 2017, these values indicate the potential amount of precipitation which can lead to flooding in the basin, this parameter is important in this research since it is an input for the design of a risk management Plan flooding in the basin.

The distribution of the storage in the soil derived from water balance modeling allows to spatially predicting that the trend is towards the occurrence of water charging towards the mountains that delimit the Pao River basin, mainly in the Northern area (Fig. 8).

By representing the data in an empirical semivariogram and adjusting it to the mathematical models used for its theoretical representation, it was possible to compare the prediction error results. For this research, the Bessel-J model was selected, representing a novelty of the method using hydrometeorological variables, since the literature reports the use of other models. This represents a contribution of this research to the understanding of this type of hydrometeorological variables, which can be applied to operating forecasts and actions of prevention of flooding in high-risk areas.

5. Conclusions

In this study, based on a spatio-temporal data modeling using satellite image analysis and processing and geostatistical methods, a spatial prediction statistical model was found for water balance variables in a basin of Venezuela. In addition, the different soil moisture conditions of the basin were combined. The results show an acceptable fit of the variables involved in the model: 1) precipitation, 2) evapotranspiration, 3) infiltration, 4) effective precipitation and 5) storage of water volume.

Spatial prediction of water balance shows a trend in the occurrence of recharge in areas north and south of the basin of the Pao River, favoring permanent water supply to three reservoirs for the purpose of supplying human located in sectors of the high, middle and lower basin of the Pao River.

The technique used for the determination of the effective rain is very useful in the forecasting of the temporal variation of the surface runoff of a basin for hydrological engineering and flood control, and identification applications of flood area. The use of remote sensing and GIS can provide the right platform to converge a great volume of multidisciplinary, being also an economic technique data. The spatial prediction statistical model of the semivariances for surface water balance (SWB) was the Bessel-J model. The correlation coefficient (R) values obtained for the statistical models of SWB spatial prediction vary according to the following ranges: precipitation 0.54-0.81; evapotranspiration 0.53-0.86; infiltration 0.68-0.95; runoff 0.68-0.92; and storage of water volume 0.53-0.95.

These values confirm that the method used to generate spatio-temporal predictions is suitable. Regarding to the evaluation of the incidence of antecedent soil moisture conditions in runoff production, the results allow to conclude that the inclusion of the antecedent moisture condition does not report significant changes in the final results for assessing surface runoff production as an important factor in hydrological studies since it determines the flooding risk factor for the communities and activities located on the floodplains of basin.

Referencias

- [1] Guevara, E. y Cartaya, H., Hidrología ambiental, Facultad de Ingeniería de la Universidad de Carabobo, Valencia, Venezuela, 2004, 166 P.
- [2] Abbott, M.B., Bathurst, J.C., Cunge, J.A., O'Connell, P.E and Rasmussen, J., An introduction to the European Hydrological System - System Hydrologique European, "SHE", 2: structure of a physically based, distributed modelling system, *J. Hydrol.* 87(1e2), pp. 61-77, 1986.
- [3] Garg, N.K. and Sen, D.J., Integrated physical based rainfall-runoff model using FEM, *J. Hydrol. Eng.*, 6(3), pp. 179-188, 2001. DOI: 10.1061/(ASCE)1084-0699
- [4] Hevesy, J.A., Istook, J.D. and Flint, A.L., Precipitation estimation in mountainous terrain using multivariate geostatistics. Part I: structural analysis. *J. Appl. Meteorol.*, 31, pp. 661-676, 1992.
- [5] Ninyerola, M., Pons, XJ., Roura, M., A methodological approach of climatological modelling of air temperature and precipitation through GIS techniques. *Int. J. Climatol.* 20, pp. 1823-1841, 2000. DOI: 10.1002/1097-0088(20001130)20:14<1823::AID-JOC566>3.0.CO;2-B
- [6] Brown, D.P. and Comrie, A.C., Spatial modeling of winter temperature and precipitation in Arizona and New Mexico, USA. *Climate Research.* 22, pp. 115-128, 2002 DOI: 10.3354/cr022115
- [7] Portuguez, D., Aplicación de la Geoestadística a modelos hidrológicos en la cuenca del río El Cañete. Tesis MSc. en Recursos Hídricos, Universidad Nacional Agraria La Molina, Perú, [en línea]. 2017, 120 P. Available at: <http://repositorio.lamolina.edu.pe/handle/UNALM/2899>
- [8] MARNR. Plan de desarrollo integral conservacionista. Ministerio del Ambiente y Recursos Naturales Renovables. Dirección Regional Cojedes, Venezuela, 1989, 328 P.
- [9] Guillén, J., Determinación de las prioridades de atención conservacionista según los riesgos de erosión actual y potencial en la cuenca del río Pao. Tesis Ing., Universidad Central de Venezuela, Venezuela, 2001, 139 P.
- [10] Giraldo, H., Introducción a la Geoestadística teórica y aplicada, Departamento Estadística, Universidad Nacional de Colombia, Bogotá, Colombia, 2002, 50 P.
- [11] Díaz, F., Evaluación de modelos geoestadísticos aplicados a la exposición al contaminante atmosférico PM10 en Chile. *Revista Ciencias Espaciales*, 8(1), pp. 441-457, 2015, DOI: /10.5377/ce.v8i1.2060.
- [12] Villareal, S. y Díaz, M., Estimación geoestadística de la distribución espacial de la precipitación media mensual y anual en Nuevo León, México (1930-2014). *Tecnología y Ciencias del Agua*, 9(5), pp. 106-130, 2018. DOI: 10.24850/j-tca-2018-05-05.
- [13] Villada, A. y Londoño, C., Aplicación de métodos geostadísticos para la caracterización de la calidad química de un depósito de material calcáreo. *Boletín Ciencias de la Tierra*, [en línea]. (35), pp. 15-24, 2014. Disponible en: <https://www.redalyc.org/articulo.oa?id=169531421002>
- [14] Domínguez, P., Cuantificación geoestadística de la contaminación por mercurio en el distrito minero de Pablo Enriquez (Provincia del Azuay), y evaluación de los impactos en el medio ambiente, Quito, Ecuador, [en línea]. 1999. Disponible en: <https://biblioteca.epn.edu.ec/cgi-bin/koha/opac-detail.pl?biblionumber=4007>.
- [15] Lloyd, C., Assessing the effect of integrating elevation data into the estimation of monthly precipitation in Great Britain, *Journal of Hydrology*, 308, pp. 128-150, 2005. DOI: 10.1016/j.jhydrol.2004.10.026
- [16] Goovaerts, P., Geostatistical approaches for incorporating elevation into the spatial interpolation of rainfall. *Journal of Hydrology*, 228, pp. 113-129, 2000. DOI: 10.1016/S0022-1694(00)00144-X
- [17] Sánchez L. y Ramírez G., Aplicación del método del intervalo de confianza como técnica geoestadística no lineal a la modelación espacial de variables geotécnicas. Colombia. *Revista DYNA*, 79(173), pp. 15-24, 2012.
- [18] Rojas, E. y Ortiz, I., Identificación del cilindro nudoso en imágenes TC de trozas podadas de Pinus Radiata utilizando el Clasificador de Máxima Verosimilitud. *Maderas, Ciencia y Tecnología*, 11(2), pp.117-127, 2009.

- [19] Lang, R., Shao, G., PijanowskI, B.C. y Farnsworth, R.L., Optimizing unsupervised classifications of remotely sensed imagery with a data - assisted labeling approach. Computers and Geosciences, 34(12), pp. 1877-1885, 2008. DOI: 10.1016/j.cageo.2007.10.011
- [20] Arango, G; Branch, B. y Botero, F., Clasificación no supervisada de coberturas vegetales sobre imágenes digitales de sensores remotos: —Landsat - ETM+|. Revista Facultad de Agronomía, Universidad Nacional de Colombia, Sede Medellin, 58(1), pp.2611-2634, 2005.
- [21] Li, M., Wu, Y. and Zhang, Q., SAR image segmentation based on mixture context and wavelet hidden - class - label Markov random field. Computers and Mathematics with Applications. 57(6), pp.961-969, 2008. DOI: 10.1016/j.camwa.2008.10.042
- [22] ENVI. User's Guide. [online]. pp. 1.177, 2005. Available at: http://www.harrisgeospatial.com/portals/0/pdfs/envi/ENVI_User_Guide.pdf
- [23] Chow, V.T., Maidment, D. y Mays, L., Hidrología Aplicada. McGraw-Hill. Santafe de Bogotá, Colombia, [en línea]. 1994. Available at: <https://baixardoc.com/documents/hidrologia-aplicada-ven-te-chow-5cae52662105a>
- [24] Parsamanesh, N., Zarrinkafsh, M., Shahoei, S.S. and Weisany, W., Evaluation of distribution functions of organic carbon with soil depth in vertisols and inceptisols. Bull. Env. Pharmacol. Life Sci, 2(12), pp. 177-183, 2013.
- [25] Voncir, N., Kparmwang, Z.T., Amba, A.A. and Hassan, A.M., Variation in morphological properties and particle size distribution of alfisols, inceptisols and entisols in the Gubi soil series, Bauchi, Nigeria. Journal of Applied Sciences, 6(13), pp. 2821-2824, 2006. DOI: 10.3923/jas.2006.2821.2824
- [26] Bremner, J.M. y Genrich, D.A., Characterization of the sand, silt, and clay fractions of some Mollisols. In: Soil Colloids and their Associations in Aggregates, Springer, Boston, MA, 1990, pp. 423-438.
- [27] Ghiberto, P., Imhoff, S., Libardi, P.L., Silva, Á.P., Tormena, C.A. and Pilatti, M.Á., Soil physical quality of Mollisols quantified by a global index. Scientia Agriculta, 72(2), pp. 167-174, 2015. DOI: 10.1590/0103-9016-2013-0414
- [28] Cerdá, J. and Villaruel, L., 2008. Evaluación de la concordancia inter-observador en investigación pediátrica: coeficiente de Kappa. Revista Chilena de Pediatría, 79(1), pp. 54-58, 2008 DOI: 10.4067/S0370-41062008000100008
- [29] Farías, B., Marquez, A., Guevara, E. y Rey, D., Caracterización espacio-temporal de usos de la tierra en la cuenca del río Pao usando técnicas de Geomáticas. Revista Ingeniería UC, [en línea]. 25(1), pp.19-30, 2018. Disponible en: <http://servicio.bc.uc.edu.ve/ingenieria/revista/v25n1/vol25n12018.pdf>
- [30] Ramirez, L.E., Development of a procedure for determining spacial and time variations of precipitation in Venezuela, Reports. Paper 145, [online]. 1971. [Fecha de consulta 05 de marzo 2018]. Disponible en: https://digitalcommons.usu.edu/water_rep/145/
- [31] Escobar, E., Evaluación del modelo de simulación SWAT para la producción de agua en una cuenca hidrográfica prioritaria de la región central de Venezuela. Caso: cuenca media del río Pao. Tesis Ing. Agrónomo. Universidad Central de Venezuela, Venezuela, 2009, 200 P.
- [32] Universidad de Carabobo, Universidad Pedagógica Experimental Libertador, Universidad Simón Bolívar, Fundación La Salle y Fundación Tierra Viva (UC, UPEL, USB, FLASA, FTV). Informe Final del Proyecto: Gestión integral de cuencas con un enfoque participativo. Casos: ríos Pao y Unare. Año 3. FONACIT. Proyecto No -2007001596. 2013.
- [33] Martelo, M., Metodología para la selección de modelos de circulación general de la atmósfera y escenarios climáticos a incluir en la primera comunicación nacional en cambio climático de Venezuela. Proyecto MARN-PNUD VEN/00/G31, Dirección de Hidrología y Meteorología, Ministerio del Ambiente y los Recursos Naturales. Caracas – Venezuela, 2003.
- [34] Guevara, E. y Márquez, A., Modelación de la infiltración en un campo agrícola de la cuenca del río Chirigua, Venezuela Revista Científica UDO Agrícola [en línea] 12(2), pp. 365-388, 2012. Disponible en: <http://www.udogricola.orgfree.com>

B.E. Farías, is an aggregate professor of Civil and Environmental Engineering at the University of Carabobo, Venezuela. She is an active researcher at the Center for Environmental and Hydrological Research of the University of Carabobo (UC-CIHAM for its acronym in Spanish). She is an active teacher at the Civil Engineering School of the University of Carabobo, Venezuela and has experience as an electromechanical civil works engineer of wastewater treatment plants. She holds a BSc. Eng. in Civil Engineer from the University of Carabobo and a MSc. in Environmental Engineering, area: environment also from the University of Carabobo in Venezuela. She is currently working on her doctoral thesis to earn her degree of Doctor (Ph.D.) in Environmental Engineering from the University of Carabobo, Venezuela. Her main area of research is environmental hydrological processes and disaster risk management.
ORCID: 0000-0002-7737-2545

A.M. Marquez-Romance, is a full professor of Civil and Environmental Engineering at the University of Carabobo, Venezuela. She is coordinator of the Center for Environmental and Hydrological Research of the University of Carabobo (UC-CIHAM for its acronym in Spanish). She is an active teacher at the Civil Engineering School and was Head of the Environmental Engineering Department of the University of Carabobo. She holds a BSc. Eng. in Civil Engineer from the University of Carabobo, a MSc. degree in Environmental Engineering and a PhD. in Engineering, Area: Environment also from the University of Carabobo in Venezuela. Her main area of research is environmental hydrological processes and environmental management. She is the author of around 30 scientific papers in technical journals and memoirs of national and international congresses and 3 textbooks.

ORCID: 0000-0003-1305-5759

E. Guevara-Pérez, is president of The National Court of Water Dispute Resolutions of the National Water Authority, Lima, Peru, and the president of the Environment and Applied Hydrology Institute (IHAMA for its acronym in Spanish). He is a member of the Engineering and Habitat Academy of Venezuela. He is a retired professor of Civil and Environmental Engineering of the University of Carabobo, Venezuela. He was coordinator of the Center for Environmental and Hydrological Research of the University of Carabobo (UC-CIHAM for its acronym in Spanish). He was General Director for Graduate Studies; Executive Director of the Council of Scientific and Humanistic Development; Head of the Department of Hydraulic Engineering of the University of Carabobo, Venezuela. He holds a BSc. Eng. in Agricultural Engineering from the National Agrarian University-La Molina, Lima, Peru, a MSc. from the Justus Liebig University, Germany, and a PhD. in Water Resource Planning from the Christian Albrecht University.

ORCID: 0000-0003-2813-2147

D.J. Rey-Lago, is a full professor of Electrical Engineering at the University of Carabobo, Venezuela, and former General Director for Graduate Studies of the University of Carabobo, Venezuela. He holds a MSc. in Computer Engineering and a Dr. of Science. His main area of research is computing science, computer architecture, high performance computing, and computer software development.

ORCID: 0000-0001-5429-5068